Simultaneous Wireless Information and Power Transfer Using Rectangular Pulse and CP-OFDM

Hussein Kassab, Jérôme Louveaux
Institute of Information and Communication Technologies, Electronics and Applied Mathematics
Université catholique de Louvain, 1348 Louvain-la-neuve, Belgium
Email: hussein.kassab@uclouvain.be; jerome.louveaux@uclouvain.be

***Abstract*—Simultaneous wireless information and power transfer (SWIPT) has recently attracted researchers and may help satisfy future technology demands. Its principle is to let wireless power transfer (WPT) and wireless information transfer (WIT) coexist based on shared resources (or sometimes even on the same signal). SWIPT can be implemented in many different ways and the literature on the topic is very wide, each solution having different obstacles. Recent studies have shown that, due to the non linearity of the rectifiers, high-PAPR waveforms provide better performance in terms of energy harvesting; hence the design of the power signal is an important issue. In addition, the presence of this power signal should consume the smallest possible amount of resources for the information transfer. In this paper, a new waveform design is proposed where the information and power signals are superposed utilizing the same frequencies at the same time. The power signal is composed of a high peak modulated rectangular wave sent during the cyclic prefix of the CP-OFDM system such that it does not interfere with the useful OFDM data symbol duration. Interference evaluation and measurements show that a good choice of signal parameters can minimize interference on the information decoder and at the same time provide good performance in terms of energy harvesting which validates the possibility of the proposed design.**

***Index Terms*—SWIPT, energy harvesting, interference, CP-OFDM, rectangular pulse, PAPR**

I. Introduction

Internet of things (IoT) electronic devices such as battery-free sensors, passive RF identification (RFID), and machine-to-machine (M2M) systems are expected to be extensively deployed in the near future. Beside their need for wireless information transfer (WIT), it is envisioned that these devices could harvest energy from the nearby electromagnetic sources or from dedicated power heads in order to extend their battery lifetime. This dual demand attracted the research community to investigate in simultaneous wireless information and power transfer (SWIPT), that considers transferring both energy and information wirelessly using the same radio frequency resources [1], [2].

SWIPT was first introduced by [3] where the fundamental trade-off between energy and information was addressed showing that the rate-energy (R-E) region is a non-increasing concave function. The work in [4] provides a comprehensive survey of state-of-art SWIPT techniques. In the signal processing and communication literature, the receiver architecture for SWIPT was proposed to be implemented in four different ways: separate receiver [5], power-splitting [6], time switching [7], or antenna switching [8].

In the early literature, no specific waveform design for the power signal was considered since the RF energy harvester was based on a linear model that depends only on the received power. Hence the power signal was usually set as a single tone. However, when the non-linearity of the rectifier is considered, it has been noticed that the efficiency of the rectifier (and output dc current) not only depends on the circuit parameters but also on the input waveform design [2], [9]. Accordingly, waveform design became an important factor that should be considered while maximizing the energy harvested. The work in [10] showed that high peak-to-average-power-ratio (PAPR) power signals provide better energy harvesting. In [2], an optimization problem was addressed using multisine waveforms to maximize the harvested dc power. Still using multisine waveforms, the work in [9] showed that there is a trade-off between the input waveform parameters, particularly the tone separation, and the receiver architecture, mainly the bandwidth of low pass filter of the rectifier.

On the other hand, several methods were proposed recently to have a combined waveform design for both power and information signals. One way to implement a combined waveform design is to divide resources either in time or in frequency which was addressed in [7], or in a time-frequency grid as proposed in [11]. Another way, proposed in [12], is to superpose a multisine power signal with a CP-OFDM information signal and use some cancellation scheme at the receiver. This has the advantage of sharing the resource simultaneously but the method might however suffer from saturation of the ADC (Analog to Digital Converter) when the power signal is of much higher level than the information signal. A different approach of combining waveforms was address in [13], where a multisine waveform is used for energy transfer with distinct levels of PAPR acting as information transfer, enabling a low-energy combined receiver.

The objective of this paper is to go further in the waveform design as well as in the WPT and WIT coexistence. Assuming that cyclic-prefix orthogonal frequency-division multiplexing (CP-OFDM) is used as multi-carrier scheme for the WIT, this paper suggests a design based on the following two facts:

This work is supported by Université catholique de Louvain under the ARC SWIPT Project.

978-1-5386-8088-9/19/$31.00 ©2019 IEEE

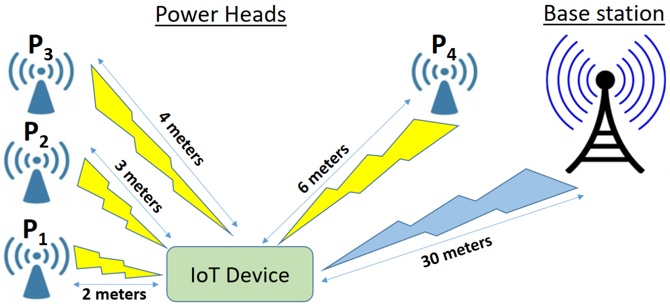

Fig. 1. Practical example of an heterogeneous network used with 4 power heads, each one transmitting an average power of 23 dBm, and potentially interfering on the information transfer between a base station, transmitting at an average power of -10 dBm, and an IoT receiver located 30 meters away.

- Higher PAPR provides better performance in terms of energy harvesting as shown by previous works [10] and confirmed by the measurements presented below.
- The cyclic prefix in the CP-OFDM system does not contain any useful information and can be discarded at the receiver for information decoding.

Therefore, the proposed idea is to design the WPT signal as a modulated rectangular wave signal that is sent during the cyclic prefix duration and is silent during the useful part of the OFDM symbol. This obviously requires some time synchronization to be implemented. But if this mild condition is satisfied, the interference created by the WPT signal on the information transfer becomes negligible, even if the power signal is of much larger amplitude. Therefore, the proposed design offers nearly perfect superposition between the WPT and WIT within the same frequency band. The IT receiver does not need to be modified with respect to a standard CP-OFDM system. The high rectangular pulses created by the WPT power heads may even simplify the synchronization of the IoT receivers. In addition, the high PAPR nature of the proposed WPT signal is shown to provide an efficient energy harvesting, even higher than a single tone with the same average power.

Although the pulse is restricted to be within the cyclic prefix duration, there might still be a small amount of interference generated by the leakage of the WPT signal into the useful OFDM data caused by channel dispersion. This interference is analyzed in detail below.

The paper is organized as follow: First, the proposed scheme and system models and waveform design are demonstrated in Section II. The computation of the interference caused by the power signal on the OFDM receiver is derived in Section III. Interference results based on a practical scenario are evaluated in Section IV. Measurements setup and results are presented in Section V. Finally, the paper is concluded in Section VI.

Notations: Scalars are noted as x, vectors are bold as $\mathbf{x}$. $*$ is the convolution operation.

II. SYSTEM MODEL

A. Wireless Network Structure

We consider an heterogeneous network that consists of a combination of the following (see an illustration in Fig.1):

- Power transmitters (or power heads)
- The information transmitter (or base station)
- The battery-free IoT device that contains:
  - A chain for information decoding
  - A chain for energy harvesting (i.e. rectifier)

It is assumed that the WIT system utilizes standard CP-OFDM as a multi-carrier scheme for data transmission between the base station and the IoT device. The useful OFDM data duration is denoted by T, and the cyclic prefix duration is dented by T_{cp}. The total number of subcarriers is denoted by N. The WPT utilizes a high-PAPR pulse $x_P(t)$ that is only transmitting power during the cyclic prefix duration. Both systems, WIT and WPT, are assumed to be precisely synchronized in time using a backhaul or any other relevant strategy. They also share the same frequency band ($\mathcal{B}$).

B. Waveform Design

The overall reasoning behind the proposed waveform design is detailed here. As already mentioned above, the goal of this design is to superpose the power and the information signals ($x_P(t)$ and $x_I(t)$) in such a way that the high power WPT signal interferes as little as possible onto the information signal. To do so, and considering that the samples within the cyclic prefix can be discarded at the receiver, the power signal is sent as a set of pulses that lie during the cyclic prefix duration (T_{cp}) only. In addition, the proposed pulsed signal generates a high PAPR waveform that is beneficial for energy harvesting as shown earlier (e.g. in [10]) and confirmed later by measurement on a energy harvesting device in section V.

The choice of the waveform pulse, that is sent during the cyclic prefix T_{cp}, should be made to reduce the risk of interference on the information signal. Particularly, the wireless channel dispersion from the power head to the IoT device causes the pulse signal to spread longer in time which may lead to interference on the previous and next OFDM symbols. Accordingly, the pulse should have the smallest possible duration in order to avoid interference on the useful OFDM symbol. On the other hand, regulations imposes that the peak power should not be more than 20 dB above the average power [14]. Hence, the best possible waveform is the rectangular shaped pulse (in equivalent baseband) where a limited average transmitted power P_{av} is utilized with a maximum possible peak during the smallest duration.

C. Power Signal Model and Parameters

As mentioned above, a power signal is generated from a power head using a modulated rectangular pulse signal that is sent only during the cyclic prefix duration T_{cp} of the n^{th} CP-OFDM total symbol ($T+T_{cp}$). Without loss of generality, we assume that the width and position of the rectangular pulse are set as multiples of the sampling time ($T_s = \frac{T}{N}$) of the signal.

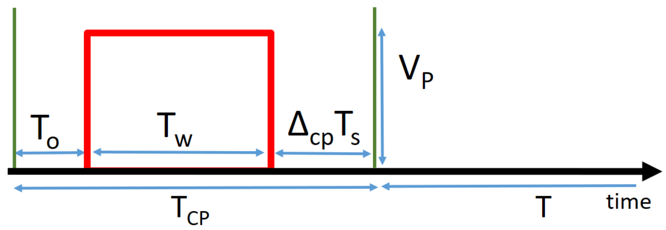

Fig. 2. Defining rectangular pulse signal parameters

Then, the baseband continuous-time signal representation of the power signal generated by any power head can be written as:

$$w_P(t) = V_p \ \text{rect}\left(\frac{t - (\frac{W_p}{2} + L_o)\ T_s}{W_p\ T_s}\right)$$
$$= \begin{cases} V_p & \text{if } \left| t - \left(\frac{W_p}{2} + L_o\right) T_s \right| \leq \frac{W_p\ T_s}{2} \\ 0 & \text{otherwise,} \end{cases} \quad (1)$$

where rect(.) is a unit square with unity duration centered around zero, and the signal parameters are defined as follows and as shown in Fig.2:

- L_o: represents the offset between the start of the cyclic prefix and the beginning of the rectangular pulse defined in terms of samples (the corresponding time is given by: $T_o = L_o\ T_s$).
- W_p: represents the width of the rectangular pulse defined in terms of samples (the corresponding time is given by: $T_w = W_p\ T_s$).
- V_p: represents the amplitude of the rectangular signal.

The total transmitted power signal generated by any given power head can be represented as:

$$x_P(t) = \sum_{n=-\infty}^{+\infty} w_P(t - n(T + T_{cp})), \quad (2)$$

where n is the index of the total OFDM symbol. To avoid interference with the useful symbol duration T, we restrict the rectangular pulse to be within the cyclic prefix duration such that $0 < L_o < L_{cp} - W_p$ where L_{cp} is the cyclic prefix duration in samples. Depending on the desired average power P_{av}, the different parameters are related by :

$$P_{av} = \frac{V_p^2 \cdot W_p}{N + L_{cp}}. \quad (3)$$

It is important to note that due to regulation constraints on the PAPR, the peak power V_p^2 may not exceed the average power by more than 20 dB. For this reason, and considering a small additional margin, we fixed the minimal value of the pulse width to

$$W_p \geq W_{p,min} = \frac{N + L_{cp}}{63} \quad (4)$$

corresponding to a maximum peak value which is roughly 18 dB higher than the average power. One important indicator is the distance between the end of the peak and the end of cyclic prefix duration L_{cp} that we refer to as "CP margin" below, and can be defined as

$$\Delta_{cp} = L_o + W_p - L_{cp}. \quad (5)$$

The CP margin Δ_{cp} , which is defined in samples, indicates how much the pulse is near or far from the next useful OFDM symbol. In practice, Δ_{cp} should be negative otherwise the rectangular pulse overlaps with the useful OFDM symbol duration creating strong interference. Therefore, most analyses below focus mostly on the absolute value $|\Delta_{cp}|$.

III. INTERFERENCE ANALYSIS

Even though we restrict the rectangular pulse to be within the cyclic prefix, interference on the useful OFDM symbol can still exist due to channel dispersion between the power head(s) and the IoT device. This interference needs to be reduced as much as possible since high power levels are radiated by the power heads that are at a close distance from the IoT device. This is usually achievable since the cyclic prefix duration (T_{cp}) is usually chosen to be large enough to accommodate for information channel dispersion which is on the same order of magnitude, or higher than the (shorter) power channel dispersion. It however still requires a careful setting of the parameters.

In this section, the interference of the rectangular wave signal on the CP-OFDM system is analyzed in detail as a function of the parameters of the system. It is important to note that this interference is in fact deterministic (up to potential synchronization errors) since the power signals are deterministic themselves. It is therefore inappropriate to use an interference evaluation based on a Power Spectral Density (PSD) model. Instead, we simply derive the interference based on the operations performed at the receiver (i.e. the filtering operations and processing done at the receiver). Then, the expressions are evaluated and the results are discussed in a practical scenario to illustrate the effect of the different parameters on this interference.

In this analysis, we assume a multipath wireless fading channel from both the power heads and the base stations towards the IoT device, and additive white Gaussian noise (AWGN). The multipath channel can be modeled as linear time-invariant filter. We directly consider the digital complex baseband equivalent channel impulse response taking into account the combination of transmit and receive filters as well as the physical channel, sampled at the sampling rate of the system $\frac{1}{T_s}$. The channel is assumed to be constant across the duration of an OFDM symbol.

We denote by $h_{P_i}[m]$ the channel experienced by the power signal from the i^{th} power head to the IoT device, and $h_I[m]$ represents the channel experienced by the information signal from the base station to the IoT device. All channels are assumed to have a maximum duration of L_{ch} taps.

The discrete time representation of the received signal at the input antenna of the CP-OFDM receiver can be expressed as follows:

$$y[m] = x_I[m] * h_I[m] + \sum_{i=1}^{U} x_P[m] * h_{P_i}[m] + w[m], \quad (6)$$

where $x_I[m]$ is the OFDM information signal and $w[m]$ is the AWGN. Assuming perfect synchronization at the information receiver chain, the cyclic prefix part is discarded from the signal. Then, the fast Fourier transform (FFT) is applied to the received windowed signal. The demodulated n^{th} symbol on the k^{th} subcarrier of the receiver can be expressed as:

$$\hat{\mathbf{d}}_k[n] = \mathbf{d}_k[n] + \sum_{i=1}^{U} \Gamma_{k,i}[n] + \mathbf{w}[n], \quad (7)$$

where $\mathbf{w}[n]$ is the filtered Gaussian noise, $\mathbf{d}_k[n]$ is the recovered symbol, and $\Gamma_{k,i}[n]$ is the interference caused by the rectangular pulse of the i^{th} power head filtered by its respective channel ($h_{P_i}[m]$) onto the k^{th} subcarrier of the n^{th} CP-OFDM symbol. Since the interference analysis is performed during one CP-OFDM symbol duration ($N + L_{cp}$), the index n can be dropped. Considering the effect of the i^{th} power head, the interference on the k^{th} information subcarrier in the digital domain can be written as:

$$\Gamma_{k,i} = \frac{V_p}{\sqrt{N}} \sum_{m=L_{cp}}^{N} \sum_{l=1}^{L_{ch}} h_{P_i}[l] \mathrm{rect}\left[\frac{m - l - \frac{W}{2} - L_o}{W_p}\right] e^{-j\frac{2\pi k m}{N}}. \quad (8)$$

Then, the total interference on the k^{th} information subcarrier coming from all power heads can be written as:

$$\Gamma_k = \sum_{i=1}^{U} \Gamma_{k,i}. \quad (9)$$

There are few comments regarding the interference analysis that are highlighted below:

- Due to the difference in travel time, power signal could potentially arrive before the information signal which will create interference onto the previous useful OFDM symbol. In this case, the rectangular peak offset L_o should be adjusted correctly to accommodate for such problem.
- High power levels of the power heads during the cyclic prefix (L_{cp}) could saturate the ADC of the information decoding chain at the IoT device. The automatic gain controller (AGC) should be designed to ignore the power received during the cyclic prefix (L_{cp}). In that case, the saturation is not problematic as the samples are discarded anyway.
- Farther power heads (or longer paths) have longer delay which could potentially spread outside the cyclic prefix duration (L_{cp}). However, they have much smaller power level and given that they are deterministic, they could be canceled out using estimation techniques. Similarly, they do not incur a high risk of ADC saturation. We do not explicitly take these cases into consideration here. This is left for further work.

TABLE I
PARAMETERS USED IN INTERFERENCE EVALUATION

CP-OFDM Parameters	
Carrier Frequency	2 GHz
Bandwidth	30.72 MHz
Sub-carrier Spacing Δ_f	15 kHz
Number of subcarriers N	2048
Sampling Period Ts	32.6 ns
Useful Symbol duration N (T)	2048 samples (66.7 s)
Cyclic Prefix duration L_{cp} (T_{cp})	144 samples (4.7 s)

Channel Indoor Parameters	
Average delay spread DS	38 ns
Delay scaling parameter r_τ	3

IV. INTERFERENCE EVALUATION

To evaluate the expression of interference above, we consider an indoor scenario with 4 power heads located at different distances from an IoT device ($d_{P_i} = 2, 3, 4, 6m$). These distances are intentionally chosen to be small so that the transmitted power remains relevant for energy harvesting at the IoT device. In addition, this can be viewed as a worst case scenario in terms of the interference these power signals can create on the information transfer. To complete the setup, the base station is located 30 meters away ($d_I = 30m$) from the IoT device. This setup is illustrated in Fig.1. The average transmitted power from every power head is assumed to be 23 dBm while the average transmitted power from the base station is considered to be -10 dBm. The parameters of the OFDM transmission (based on an LTE scenario) are provided in Table I along with the channel parameters used in this evaluation. They are based on an "Indoor office" model extracted from the WINNER II Channel Models [15]. The delay scaling parameter r_τ controls the rate of decay of the power delay profile. Based on these, 4 different power delay profiles have been randomly generated and associated with the 4 different power heads. They are represented in Fig.3. Those profiles are kept constant for all simulations presented below. Each simulation is based on 2000 independent channel realizations generated from the power delay profiles represented in Fig. 3. The channel impulse response takes into account the transmit and receive filters in addition to the physical channel.

Fixing the pulse offset to L_o and the pulse width to W_p, the total interference onto every subcarrier (summed over the contributions of all power heads) is computed and averaged over 2000 realizations. The results are shown in Fig.4 for 4 different sets of parameters. We notice that the interference values can vary across subcarriers with various patterns depending on the parameters. In order to be able to compare more easily the effects of the different parameters, this interference is then further averaged over the subcarriers.

To highlight the importance of the CP margin $|\Delta_{cp}|$ on the interference, we first fix the pulse offset to $L_o = 31$ samples and vary the rectangular pulse width W_p to evaluate the average interference caused by these power heads onto the useful OFDM symbol. This average interference is represented

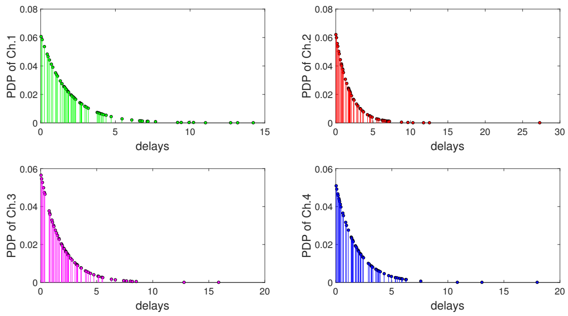

Fig. 3. Power delay profiles for the channels of the power heads based on Indoor office model (total energy normalized to 1).

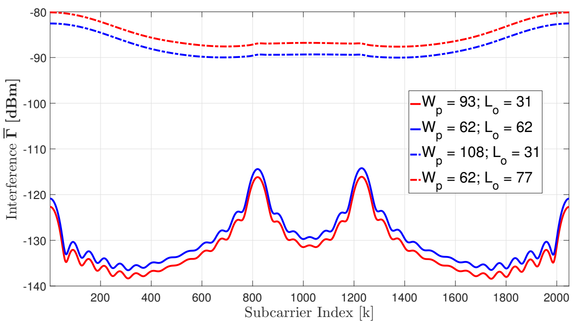

Fig. 4. Interference per subcarrier averaged over 2000 channel realizations when $\Delta_{cp} = -20$ for ($L_o = 31$, $W_p = 93$) and ($L_o = 62$, $W_p = 62$); and when $\Delta_{cp} = -5$ for ($L_o = 31$, $W_p = 108$) and ($L_o = 77$, $W_p = 62$)

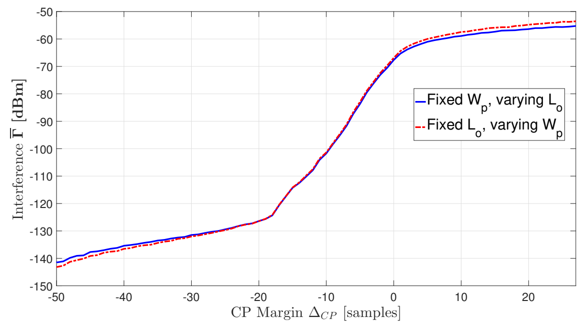

Fig. 5. Average interference as function of Δ_{cp}. The continuous line corresponds to $L_o = 31$ samples and varying W_p while the dotted line corresponds to $W_p = 93$ samples and varying L_o

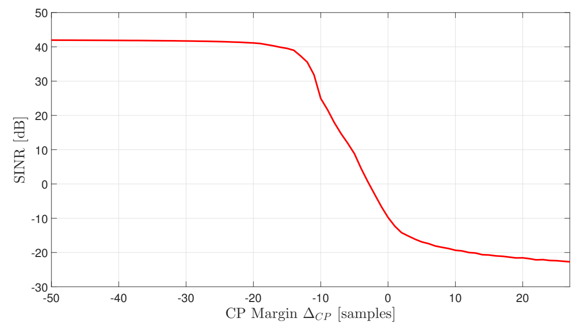

Fig. 6. SINR of the information signal for different values of Δ_{cp}

in Fig.5 as a function of the CP margin Δ_{cp}, which directly varies with the width W_p. As expected, this figure shows that interference increases when the CP margin $|\Delta_{cp}|$ decreases. In other words, the farther the pulse is from the edge of the cyclic prefix, the lower the interference is (except obviously when Δ_{cp} becomes positive). On another hand, the interference is then evaluated with a fixed pulse width $W_p = 93$ and a varying pulse offset L_o. The results are also shown in Fig.5 as a function of the CP margin Δ_{cp}, which also directly varies with the pulse offset L_o. Both curves exhibit very similar behavior, proving that the CP margin is the main parameter affecting the interference. In particular, the changes to the peak voltage (that are related to the pulse width W_p to maintain a fixed average power) are negligible with respect to variations of the CP margin Δ_{cp}. Hence, regardless of whether the width or the offset is varying, we can approximate that the interference is a direct function of the CP margin Δ_{cp}. To further confirm the result, Fig. 4 plots the per-subcarrier interference for four sets of parameters where each couple of parameters corresponds to the same CP margin Δ_{cp}. Once again, the curves exhibit very similar behaviors with slight differences which are related to the change in the pulse height V_p while varying W_p.

In order to evaluate the potential performance loss of the information transmission, we computed the SINR (signal-to-interference and noise-ratio) at the IoT device for the considered setup, based on the powers transmitted by the different nodes, and taking into account the path losses. The SINR is illustrated in Fig.6 as a function of the CP margin Δ_{cp}. As expected, increasing the absolute margin $|\Delta_{cp}|$ is beneficial for the performance of the information transmission. It can also be observed that, with the proposed setup, low interference levels (SINR > 30 dB) can easily be obtained with a margin of $\Delta_{CP} = -20$ samples, for instance with $L_o = 31$, which provides a good protection against synchronization errors, and with $W_p = 93$ which is already much higher than the minimum value ($W_{p,min} = 35$ for this setup) related to the peak power regulations. This leads to a negligible interference even in the scenario considered here, where the power heads are close to the IoT device.

V. MEASUREMENTS

In the previous section, the impact of the power signal on the data was analyzed. In this section we focus on the effect of the pulse choice on energy harvesting. As mentioned in the introduction, our choice of the power signal is based on the fact that high PAPR signals provide better energy harvesting efficiency. In order to confirm this we have conducted a series of measurements on a real RF energy harvesting device. This device was designed and manufactured by the ECS Group in the ICTEAM institute at UCLouvain [16]. It uses a Greinacher rectifier with a π matching network. A universal software radio peripheral (USRP) device was used to generate and transmit the modulated rectangular signal based on the

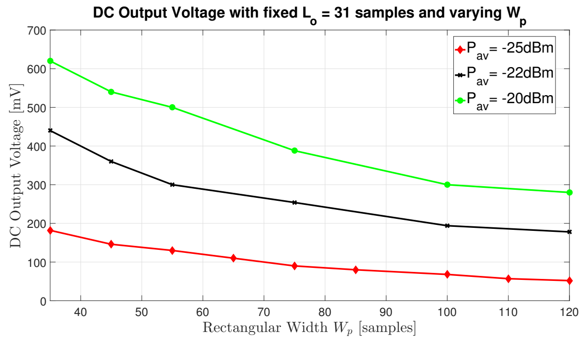

Fig. 7. Measurement results for DC output voltage versus the CP margin Δ_{cp} for average transmitted powers -25 dBm, -22 dBm, and -20 dBm

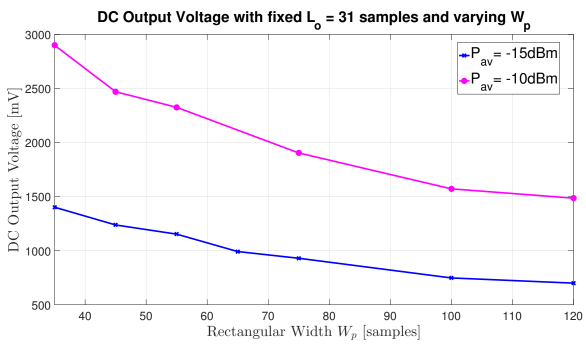

Fig. 8. Measurement results for DC output voltage versus the CP margin Δ_{cp} for average transmitted powers -15 dBm and -10 dBm

parameters shown in Table I. The USRP and the rectifier are connected back-to-back using RF coaxial cable. Then, the DC output voltage at the output of the rectifier is measured using an oscilloscope. The objective of these measurements is to observe the influence of the signal parameters on the amount of harvested energy. Considering a fixed transmitted average power P_{av}, the only parameter that can potentially affect the harvested energy is the width of the rectangle W_p, since the peak value V_p is induced by 3. Obviously, a time shift in the power signal, i.e. the offset L_o, does not affect the amount of harvested energy. The DC voltage at the output of the RF rectifier was measured for different values of the pulse width W_p and for different average transmitted powers P_{av}. The measurement results are shown in Fig.7 and Fig.8.

The results show that the harvested DC voltage increases when the width of the pulse decreases (which results in a higher pulse). In other words, given a certain amount of average transmitted power, high PAPR signals provide better performance in terms of energy harvesting. As a result, it is interesting to stress that narrow pulses provide better performance both in terms of energy harvesting (i.e higher PAPR) as well as interference on the information transfer as shown in section IV. This confirms the choice of having a rectangular pulse power signal which should be as short as possible. As mentioned above, this is of course limited by the peak power regulations.

VI. CONCLUSION

This work proposes a novel technique that allows WIT and WPT to coexist with essentially no degradation of their respective performance as long as a good time synchronization is kept. The proposed waveform is a modulated rectangular pulse that is sent during the cyclic prefix of the CP-OFDM information system. Given a limited amount of transmitted power, the interference evaluation and energy harvesting measurements show that a short pulse with a sufficient offset L_o (to counter any delay difference or synchronization issues) provide good energy harvesting performance as well as significantly reduce the amount of interference caused by the power signal onto the information signal. The pulse itself may even help the synchronization of the different devices in the system. The results are promising but the technique still requires further practical validation using hardware.

REFERENCES

[1] Y. Zeng, B. Clerckx, R. Zhang, "Communications and signals design for wireless power transmission," IEEE Trans. Commun., vol. 65, no. 5, pp. 2264–2290, Mar. 2017.
[2] B. Clerckx and E. Bayguzina, "Waveform design for wireless power transfer," IEEE Trans. Signal Process., vol. 64, no. 23, pp. 6313–6328, Dec. 2016.
[3] L. R. Varshney, "Transporting information and energy simultaneously," in Proc. Int. Symp. Inf. Theory, pp. 1612–1616, Jul. 2008.
[4] T. Perera, D. Jayakody, S. Sharma, S. Chatzinotas, and J. Li, "Simultaneous Wireless Information and Power Transfer (SWIPT): Recent Advances and Future Challenges," IEEE Commun. Surveys and Tutorials, vol. 20 , no. 1, pp. 264–302, Dec. 2017.
[5] R. Zhang and C. K. Ho, "MIMO broadcasting for simultaneous wireless information and power transfer," IEEE Trans. on Wireless Commun., vol. 12, no. 5, pp. 1989–2001, 2013.
[6] X. Zhou, R. Zhang, and C. K. Ho, "Wireless information and power transfer: Architecture design and rate-energy tradeoff," IEEE Trans. Commun., vol. 61, no. 11, pp. 4754–4767, Nov. 2013.
[7] X. Zhou, R. Zhang, and C. K. Ho, "Wireless information and power transfer in multiuser OFDM systems," IEEE Trans. Wireless Commun., vol. 13, no. 4, pp. 2282–2294, Apr. 2014.
[8] K. Huang and E. G. Larsson, "Simultaneous information and power transfer for broadband wireless systems," IEEE Trans. Signal Process., vol. 61, no. 23, pp. 5972–5986, Dec. 2013.
[9] N. Pan, M. Rajabi, and N.B. Carvalho, "Bandwidth Analysis of RF-DC Converters Under Multisine Excitation," IEEE Trans. Microw. Theory Techn., vol. 66, no. 2, pp. 791–802, Feb. 2018.
[10] C. R. Valenta, M. M. Morys, and G. D. Durgin, "Theoretical energy-conversion efficiency for energy-harvesting circuits under power optimized waveform excitation," IEEE Trans. Microw. Theory Techn., vol. 63, no. 5, pp. 1758–1767, May 2015.
[11] H. Kassab and J. Louveaux, "Gabor Expansion for Simultaneous Wireless Power and Information Transfer (SWIPT): Interference Analysis," in Proc. of the 39th Symp. on Inf. Theory and Signal Process. in the Benelux, pp. 847–862, June 2018.
[12] B. Clerckx, "Wireless Information and Power Transfer: Nonlinearity, Waveform Design, and Rate-Energy Tradeoff," IEEE Trans. Signal Process., vol. 66, no. 4, pp. 847–862, Feb. 2018.
[13] D. I. Kim, J. H. Moon, and J. J. Park, "New SWIPT using PAPR: How it works," IEEE Wireless Commun. Lett., vol. 5, no. 6, pp. 672–675, Dec. 2016.
[14] Rules and regulations of "Federal Communication Commission (FCC)", codified in Title 47 of the Code of Federal Regulations (CFR), Part 15.
[15] P. Kyosti et al., "Part 1: Channel Models," WINNER II Project D1.1.2 V1.1, version 1.1, Nov. 2007.
[16] R. Dekimpe, P. Xu, M. Schramme, D. Flandre and D. Bol, "A Batteryless BLE IoT Motion Detector Supplied by 2.45-GHz Wireless Power Transfer," in: IEEE (Ed.), Power and Timing Modeling, Optimization and Simulation, 28th International Symposium on, pp. 68–75, Jul. 2018.